analytical chemistry

Article

pubs.acs.org/ac

Mechanism of Ion Transfer in Supported Liquid Membrane Systems: Electrochemical Control over Membrane Distribution

Matěj Velický,[†] Kin Y. Tam,[‡] and Robert A.W. Dryfe*[,†]

[†]School of Chemistry, University of Manchester, Oxford Road, Manchester M13 9PL, United Kingdom

[‡]Faculty of Health Science, University of Macau, Macau, China

Supporting Information

ABSTRACT: A polarization study carried out on a thin supported liquid membrane separating two aqueous compartments is presented. Transfer of both the ionized and uncharged form of an organic tracer dye, rhodamine B ([9-(2-carboxyphenyl)-6-diethylamino-3-xanthenylidene]-diethylammonium chloride), across supported liquid membranes composed of one of 1-octanol (octan-1-ol), 1,9-decadiene (deca-1,9-diene), 1,2-dichlorobenzene, or nitrophenyl octyl ether (1-(2-nitrophenoxy)octane) was studied using cyclic voltammetry and UV−vis absorption spectrophotometry. Concentration analysis indicates that the high membrane concentration of rhodamine B determines the ionic transfer observed via voltammetry, which is consistent with the low aqueous ionic concentration and large membrane/aqueous distribution of the molecule. The observed double-transfer voltammogram, although it has been largely neglected in previous literature, is a logical consequence of the presence of two liquid−liquid interfaces and is rationalized in terms of ion transfer across the two interfaces on either side of the membrane and supported by voltammograms obtained for a series of ions of varied lipophilicity. The bipolar nature of the voltammetric response offers an effective way of mass transport control via changing polarity of the applied voltage and finds immediate use in extraction, purification, and separation applications.

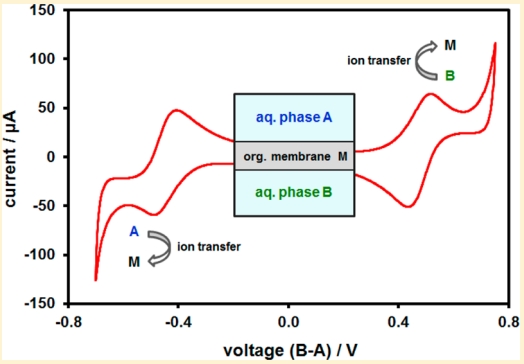

Supported liquid membranes (SLM) are composed of a solvent immobilized on a polymer membrane, which separates two (usually aqueous) solution phases. They have found use in liquid−liquid extraction,[1] ion-selective electrodes (ISE),[2] pharmaceutical research as mimics of biological membranes,[3] and the partitioning of actinides.[4] Some of the SLM applications include use of an electrical field to modulate the membrane's physicochemical properties.[5] Conceptually, the application of electrochemistry to a SLM can be viewed as a bipolar version of liquid−liquid electrochemistry, normally performed at the interface between two immiscible electrolyte solutions (ITIES).[6] The connection between SLMs and electrochemistry at the ITIES motivated various groups to explore the analogue between the two techniques.

Samec et al. studied ionized drug transfer across an SLM using voltammetry[7] and also developed theory to support the observed current−potential dependence.[8] Ulmeanu et al. used a commercial 96-well microfilter plate system to study partitioning of ionized drugs across a SLM[9] and the transfer of highly hydrophilic ions[10] in a system where only one of the SLM interfaces is polarizable via use of a common partitioning ion. Murtomäki et al. studied transfer of tetraalkylammonium cations across an SLM in the rotating diffusion cell.[11] Furthermore, an extensive theoretical description of the SLM systems supported with experimental observations was reported by Molina et al.[12,13] Electrochemistry on SLM systems is usually performed using a four-electrode setup, i.e., a pair of reference and counter electrodes placed in each aqueous phase, which is typical for thin membranes (on the order of 10−100 μm). A more advanced technique, using a six-electrode setup, was presented by Kihara and co-workers for thicker membranes (10 mm), where another pair of electrodes was placed in the membrane phase.[14] Many research activities have focused on application of SLMs to ISE potentiometry.[15,16]

The choice of membrane solvents comes from their varied application and/or relevance to SLM systems. 1-Octanol (commonly known as *n*-octanol) has become a standard solvent for drug candidate lipophilicity determination and prediction of absorption in humans.[17,18] Whereas the low polarity of 1-octanol requires specific electrochemical experiments,[19,20] 1,2-dichloroethane (DCE) combines suitable pharmaceutical relevance with good physical properties and has thus become a popular choice for liquid−liquid electrochemistry.[21,22] However, DCE is not suitable for thin-layer SLMs, due to its relatively high miscibility with water. A good alternative to DCE is 1,2-dichlorobenzene (ODCB), since its miscibility with water is lower and it also poses a lower health hazard than DCE. ODCB has been used in SLM applications for transfer of both organic[23] and inorganic[24] species as well as for ion transfer using electrochemical methods.[25] A solvent of

Received: July 26, 2013
Accepted: December 3, 2013
Published: December 3, 2013

   dx.doi.org/10.1021/ac402328w | *Anal. Chem.* 2014, 86, 435−442

pharmaceutical relevance, which has been used as a biological membrane mimic, is 1,9-decadiene.[26−28] It has been shown recently that polarization of an SLM with 1,9-decadiene as a membrane solvent is possible.[29] Finally, nitrophenyl octyl ether (NPOE) is a solvent widely used in liquid−liquid electrochemistry,[30] electro-kinetic extraction of drugs,[5,31] ion-selective electrodes,[32] and both passive[33] and electrochemically controlled[34] drug transfer across SLMs. Herein, the SLM system was studied using cyclic voltammetry and spectrophotometry using four membrane solvents, 1-octanol, 1,9-decadiene, ODCB, and NPOE.

The aim of this manuscript is to elucidate the transport of ionized species across supported liquid membranes using cyclic voltammetry and spectrophotometry. Challenging properties of the transfer, such as the direction and extent of the diffusion, concentration distribution, and dissociation equilibrium, were studied using a model molecule, rhodamine B [9-(2-carboxyphenyl)-6-diethylamino-3-xanthenylidene]-diethylammonium chloride. Rhodamine B (RB) is a xanthene derived fluorescent dye with strong UV−vis absorption used predominantly as a tracer in biotechnology applications.[35−38] Permeability of RB was previously studied in pharmaceutical research[39] and wastewater treatment applications.[40] The molecule contains amino- and carboxy-functional groups, is predominantly uncharged in the aqueous phase at neutral pH, being a weak base with pK_a value of 3.2−3.7,[41,42] and has an aqueous diffusion coefficient of 4.27×10^{-6} cm^2 s^{-1}.[43] A large distribution coefficient of RB between the membrane and aqueous phase and the small fraction of RB^+ cations (∼0.05% at pH = 7) in the aqueous phase results in membrane "sink" conditions. The high concentration of RB (and RB^+) within the membrane dominates the voltammetric response and shows inversely driven transfer, i.e., out from the membrane phase.

Most interestingly, rhodamine B voltammetry across the SLM exhibits a double-transfer feature, which as shown below, is attributed to separate transfers at the two ITIES. The double-transfer voltammogram, which is also presented for a range of other cations and anions of varied lipophilicity, has important consequences for many SLM applications, such as extraction, separation, and purification as discussed below.

EXPERIMENTAL SECTION

Reagents and Materials. Sodium dihydrogen phosphate (98.5%), rhodamine B ([9-(2-carboxyphenyl)-6-diethylamino-3-xanthenylidene]-diethylammonium chloride, fluorescence grade), 1,9-decadiene (98%), tetramethylammonium chloride (99%), tetraethylammonium chloride hydrate (≥98.5), tetrabutylammonium chloride (99%), crystal violet (tris(4-(dimethylamino)phenyl)methylium, VETRANAL), sodium tetrafluoroborate (≥98.5), sodium perchlorate (99%), sodium dodecylsulfate (≥97%), tetradodecylammonium chloride (≥97%), tetradodecylammonium tetrakis(4-chlorophenyl)-borate (≥98%), 1-octanol (octan-1-ol, ≥99%), 1,9-decadiene (deca-1,9-diene, 98%), 1,2-dichlorobenzene (99%), and nitrophenyl octyl ether (1-(2-nitrophenoxy)octane, ≥99%) were purchased from Sigma-Aldrich, U.K., and used as received. Potassium chloride (99%), sodium chloride (99.95%), sodium hydroxide (98.8%), and hydrochloric acid (analytical reagent grade, 38%) were obtained from Fisher Scientific UK Ltd. Deionized water, of 18.2 MΩ cm resistivity, purified by a "PURELAB" Ultrafiltration unit (Elga Process Water, Marlow, U.K.) was used for solution preparation. Membranes were made from "Durapore" Poly(vinylidene fluoride) (PVDF) hydrophobic membrane filters (0.45 μm pore size, 125 μm thickness, 75% porosity, 13 mm diameter) supplied by Millipore and attached to a ground glass tube, denoted A (Glass Precision Engineering Ltd., Leighton Buzzard, U.K.), using Araldite Rapid glue (Bostik Ltd., Stafford, U.K.; see Figure 1). The polytetrafluoroethylene (PTFE) cell, denoted B,

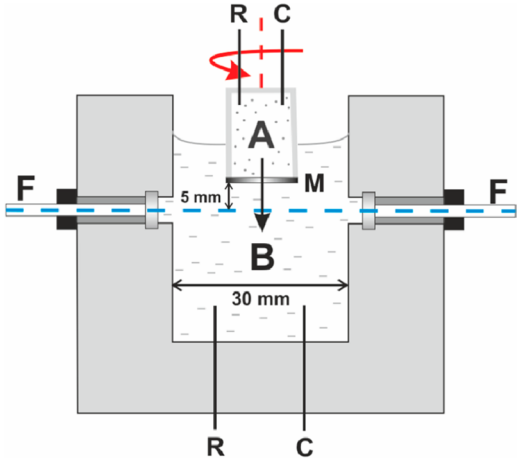

Figure 1. Schematic of the SLM system with electrochemical and UV−vis detection: A, aqueous phase "A"; B, aqueous phase "B"; M, supported liquid membrane; F, fiber-optic cable; C, platinum counter electrode; R, Ag/AgCl reference electrode (saturated KCl internal solution). The red arrow/line indicates the axis of membrane rotation, and the blue line shows the UV−vis optical path.

with fiber-optic fittings was made in-house. The Ag/AgCl reference electrodes were made by oxidation of a silver wire in 0.1 M potassium chloride solution, at a current density of 5×10^{-3} A cm^{-2}, and enclosing the wire in saturated KCl solution separated from the system by a "Vycor" porous glass frit (3 mm diameter, SciMed Ltd., Cheadle, U.K.). Platinum wire (0.5 mm diameter, 99.99%) and platinum mesh (0.1 mm plain weave wire, 420 per cm^2, open area 62.7%) were used for counter electrode preparation. All metals were obtained from Advent Research Materials (Oxford, U.K.).

Apparatus. The experimental setup was described in detail previously.[29] A schematic diagram of the SLM system with embedded apparatus for simultaneous electrochemical and *in situ* UV−visible detection is depicted in Figure 1. The system consists of two cells, A and B, which contain the buffered aqueous phase with electrolyte and are separated by a supported liquid membrane. The PTFE cell B was fitted with the fiber-optic and connected to a UV−vis absorption spectrometer (DH-2000-BAL, supplied by Ocean Optics, Duiven, The Netherlands) equipped with a DH-2000-BD deuterium bulb, DH-2000-BH tungsten halogen bulb, and USB2000 interface (Micropack GmbH, Ostfildern, Germany). Sodium phosphate was used as a buffer to maintain pH 7.0, and sodium chloride is used as electrolyte to support current flow in the aqueous phase. Tetradodecylammonium tetrakis(4-chlorophenyl)borate ($TDDATPBCl_4$) was added to the membrane solvent as the electrolyte for the organic phase. Rhodamine B was the primary analyte for the transfer across the SLM. Tetramethylammonium (TMA^+), tetraethylammonium (TEA^+), tetrabutylammonium (TBA^+), and crystal violet (CrV^+) purchased as chloride salts and tetrafluoroborate (BF_4^-), perchlorate (ClO_4^-), and dodecylsulfate (DS^-) purchased as sodium salts were also used as analytes. Each

dx.doi.org/10.1021/ac402328w | Anal. Chem. 2014, 86, 435−442

aqueous phase contained a pair of counter and reference electrodes (denoted C and R), to allow the polarization of the SLM. Each counter−reference electrode pair was connected together via a 100 nF capacitor to reduce externally induced electrical noise (Farnell, Leeds, U.K.). The four electrodes were connected to the potentiostat/galvanostat (Autolab PGSTAT 100, Metrohm-Autolab BV, Utrecht, The Netherlands) with polarity corresponding to the potential difference between the aqueous phases B and A, $\Delta E_{B/A}$. The two organic/aqueous interfaces have geometric membrane areas (total area × porosity) of 0.59 cm^2 (SLM/phase A) and 0.78 cm^2 (SLM/phase B) giving an averaged membrane area of 0.68 cm^2 (different areas are the result of membrane attachment to the glass donor tube; see Figure 1). Rotation at 200 rpm (21 rad s^{-1}) of the membrane was applied in some cases. This was controlled using a Model 616 rotating-disc controller (EG&G Parc). Solution pH was measured using a HI991300 pH meter (Hanna Instruments).

The composition of the supported liquid membrane cell can be described as follows: Ag(s)|AgCl(s)|KCl(sat.)|10 mM NaH_2PO_4, 10 (or 100) mM NaCl, *x*RB (TMA^+, TEA^+, TBA^+, CrV^+, BF_4^-, ClO_4^-, DS^- at 1 mM), pH 7.0 (aq) ‖ 10 mM $TDDATPBCl_4$ (1-octanol, 1,9-decadiene, ODCB or NPOE) ‖ 10 mM NaH_2PO_4, 10 (or 100) mM NaCl, *y*RB (TMA^+, TEA^+, TBA^+, BF_4^-, ClO_4^-, DS^- at 1 mM), pH 7.0 (aq)|KCl(sat.)|AgCl(s)|Ag(s).

Where x and y are in the range of 0−100 μM. High conductivity of the aqueous phase implies that the system resistivity varies depending on the membrane solvent. Internal IR compensation was applied for each solvent system in order to compensate for the current induced by the applied potential difference due to resistance of the system (1,9-decadiene ∼ 45−55 kΩ; 1-octanol ∼ 8−9 kΩ; ODCB ∼ 2−3.5 kΩ; NPOE ∼ 2−3 kΩ). The resistivity value of the membrane was determined from the resistance measured via potentiostat and the membrane thickness. A two phase shake-flask method and UV−vis spectrophotometry was used to determine the distribution of RB between the organic and aqueous phase.

RESULTS AND DISCUSSION

Rhodamine B Permeability and Distribution Across the SLM. Rhodamine B, added to aqueous phase A at a concentration of 100 μM, permeates through the SLM due to the concentration gradient between the aqueous phases. The permeation rate is governed by the diffusion coefficients in the aq. phase and the membrane, membrane/aqueous distribution coefficient, concentration equilibrium, and extent of stirring. The SLM was rotated about its vertical axis, as indicated in Figure 1, maintaining stable hydrodynamic conditions on both sides of the membrane and uniform mixing of both the aqueous phases. The permeation of RB across a nonpolarized SLM containing one of the four solvents, 1-octanol, 1,9-decadiene, ODCB, or NPOE, at a constant stirring rate of 200 rpm (21 rad s^{-1}) is shown in Figure 2. Rhodamine B absorbs strongly in the visible region (maximum absorption coefficient of 8.79 × 10^4 M^{-1} cm^{-1} at 555 nm, aqueous pH 7.0), and therefore, the appearance of the molecule in phase B can be monitored (inset of Figure 2). RB was stable under UV−vis light as shown in the Supporting Information (S-2).

The effective permeability coefficients, P_e, were determined from the concentration−time profile as described elsewhere.[27,29] Briefly, the time-dependent concentration in phase B was transformed into a function, k, also depending on the initial analytical (total) concentration in phase A and the volumes of both the aqueous phases. The logarithm of this function changes linearly with time, t, after a steady-state diffusion profile has been established across the three phases:

$$\ln(k) = -at \tag{1}$$

where a is defined as follows:

$$a = \frac{AP_e}{V_D}\left(1 + \frac{V_D}{V_A}\right) \tag{2}$$

where A is the membrane area, and V_D and V_A are the donor and acceptor phase volumes, respectively.

In the case of "infinite" stirring, i.e., when the aqueous diffusion layer is compressed to zero, the aqueous analytical concentrations c_A and c_B are uniform throughout the phases A and B, respectively, and the membrane concentration changes linearly inside the membrane as depicted in a qualitative schematic in Figure 3 (black solid lines). The membrane and aqueous concentrations are related via distribution coefficient, K_d:

$$K_d = \frac{c_{M,A}}{c_A} = \frac{c_{M,B}}{c_B} \tag{3}$$

where $c_{M,A}$ and $c_{M,B}$ denote the steady-state concentrations of RB in the membrane near the interface with phases A and B, respectively. The distribution coefficient, K_d, of rhodamine B between the organic phase and aqueous phase was determined using the standard shake-flask method. For a general case of a finite stirring rate, the aqueous concentration near the membrane changes according to diffusion laws, resulting in an altered steady-state profile as depicted by the blue dashed curves in Figure 3. Therefore, in reality, the membrane interfacial concentrations will be slightly lower ($c_{M,A}$) and higher ($c_{M,B}$), respectively, as demonstrated by the blue dashed line in Figure 3. Steady-state conditions at any stirring rate, i.e., an approximately linear concentration profile within the membrane, allow the mean membrane concentration, c_M, to be calculated as a simple arithmetic average of $c_{M,A}$ and $c_{M,B}$.

The extent of analyte permeation varies significantly with the membrane solvent used as Figure 2 shows. The 1,9-decadiene

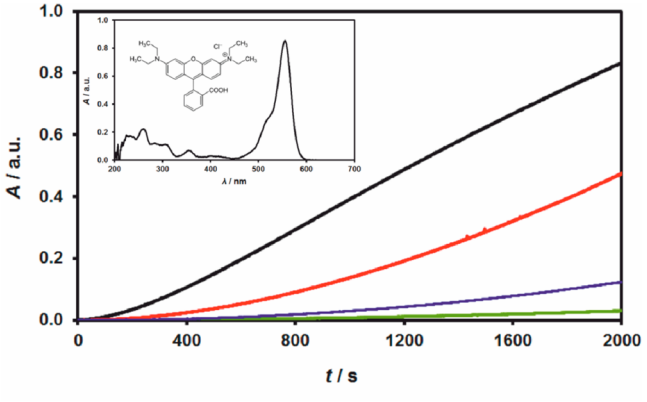

Figure 2. Hydrodynamically controlled permeation of rhodamine B across a nonpolarized SLM rotated at 200 rpm (21 rad s^{-1}). RB was initially present in the aq. phase A only (x = 100 μM). The absorbance at wavelength of 555 nm in aq. phase B is recorded with time for the four solvents: black, 1,9-decadiene; red curve, 1-octanol; blue curve, NPOE; green curve, ODCB. The inset graph shows a UV−vis spectrum of 3 μM RB in the aqueous phase at pH 7.0.

dx.doi.org/10.1021/ac402328w | Anal. Chem. 2014, 86, 435−442

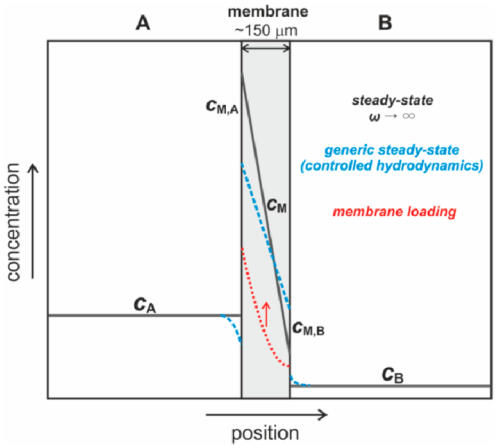

Figure 3. A qualitative schematic showing the concentration profile of a model molecule (K_d = 3) across the supported liquid membrane system with concentration gradient between the phases A and B. The black solid lines represent the aqueous steady-state concentrations, c_A and c_B, and the average membrane steady-state concentration c_M for an ideal case of "infinite" stirring of the aqueous phases; $c_{M,A}$ and $c_{M,B}$ denote the steady-state concentrations in the membrane near the interface with phases A and B, respectively. Blue curves represent a generic steady-state profile of finite aqueous stirring, and the red curve represents the transient membrane loading effect.

system has the fastest permeation of RB across the SLM, followed by 1-octanol and NPOE. ODCB exhibits the slowest membrane permeation of the analyte. The permeability and distribution coefficient data (Table 1) show the opposite trend to that normally expected; i.e., here, the highest distribution coefficient corresponds to the lowest permeability. This is rationalized in terms of a membrane loading effect (lag-time period before the concentration steady-state is reached), typical for molecules with a large distribution coefficient.[44] The high affinity of RB for the organic phase means large amounts of the molecule must be transferred to the SLM in order to reach steady-state concentration. Consequently, the appearance of the molecule in phase B is slower, and the time needed before the steady-state is reached increases as depicted by the red dotted curve in Figure 3.

In fact, the rapid depletion of phase A in favor of the SLM provides membrane sink conditions as shown by the concentration analysis. The steady-state concentration distribution between the aqueous phases and the membrane, determined from the UV–vis measurement, and distribution coefficient and mass balance is summarized in Table 1. The concentration profile in the phase A–SLM–phase B system was a basis for the analysis and rationalization of the observed RB^+ transfer across the double ITIES (see below).

Transfer of Rhodamine B across the SLM Using Voltammetry. SLMs were formed using the group of four organic solvents (1-octanol, 1,9-decadiene, ODCB, or NPOE), and the transfer of the rhodamine B cation (RB^+) was studied using voltammetry. 1,9-Decadiene, ODCB, and NPOE SLMs exhibit a large potential window of about 1.2 V centered around 0 V, which is suitable for transfer of ions within this potential range. 1-Octanol did not prove to be suitable for voltammetry due to its high resistivity and narrow potential window. Comparison and analysis of the analyte-free (blank) spectroelectrochemical data for all four solvents is shown in the Supporting Information (S-3). The changes in UV–vis absorption of RB^+ induced by polarization are negligible compared to the permeation fluxes, and therefore, monitoring of the concentration changes via spectrophotometry was not possible.

Figure 4a shows cyclic voltammograms obtained for each solvent system after the nonpolarized permeation (Figure 2) was completed, i.e., when the analyte flux has reached a steady-state. Two pairs of the observed transfer peaks, symmetrical about the zero potential difference axis, are observed for all the solvents, except 1-octanol, are attributed to the double transfer of the analyte across the respective interfaces, and are discussed in detail below. Several conclusions can be deduced from the size of the current, shape of the voltammogram, and difference between the three membrane solvents, where double transfer was seen (i.e., 1,9-decadiene, ODCB, and NPOE).

First, although the observed voltammogram has a shape intermediate between a peak-shape and a limiting current plateau, even though the aqueous phases on both sides of the membrane had mass transport controlled via stirring,[45] the voltammograms carried out under stagnant aqueous conditions did not reveal a substantial change in the peak size. Furthermore, changes in the stirring rate had a limited effect on the peak current. This indicates that the observed transfer of RB^+ via applied potential is predominantly governed by the transport in the stagnant membrane phase.

In other words, the observations indicate that peaks 1 and 3 correspond to transfer of RB^+ cation out of the membrane to aqueous phases B and A, respectively, according to the applied potential difference between B and A. This transfer is most likely coupled to the cotransport of the membrane anion ($TPBCl_4^-$) out of/into the membrane as indicated in Figure 4a (detailed analysis of the coupled transfer mechanism is given in the Supporting Information, S-4).

Table 1. Permeability Coefficients, Distribution Coefficients, and Steady-State Analytical Concentrations of Rhodamine B in the Aqueous Phases and SLM[a]

SLM solvent	$P_e/10^{-5}$ cm s^{-1}[b]	K_d[c]	$c_A/\mu M$[d]	$c_B/\mu M$[d]	$c_{M,A}$/mM[e]	$c_{M,B}$/mM[e]	c_M/mM[f]
ODCB	2.7	2864	25.0	0.1	71.4	0.4	35.9
NPOE	12.1	839	52.4	0.5	44.0	0.4	22.2
1-octanol	43.4	232	78.3	1.9	18.2	0.4	9.3
1,9-decadiene	48.8	64	90.4	3.9	5.8	0.2	3.0

[a]Determined near the end of permeation, i.e., assuming analyte flux has become constant. [b]Permeability coefficient determined from concentration–time measurement and eq 1. [c]Distribution coefficient between the membrane and aqueous phase from the shake-flask method. [d]Analytical concentrations in aqueous phases A and B, respectively, measured via UV–vis absorption. [e]Analytical concentration in the membrane phase, at the interface with phase A and B, respectively, calculated from eq 3. [f]Average analytical concentration in the membrane phase, calculated as an arithmetic average of $c_{M,A}$ and $c_{M,B}$.

dx.doi.org/10.1021/ac402328w | Anal. Chem. 2014, 86, 435–442

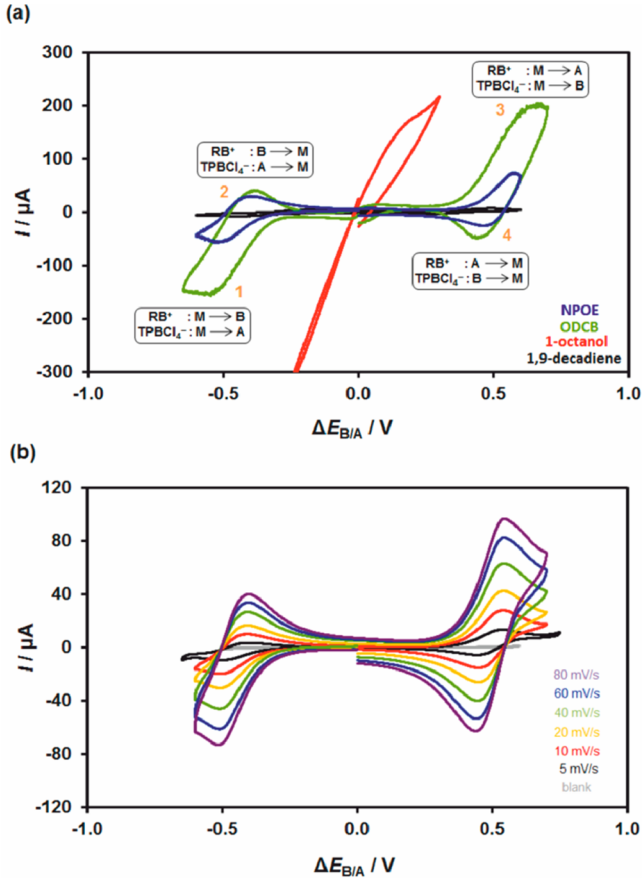

Figure 4. Voltammetry of rhodamine B transfer across the SLM system as a function of applied potential difference between phases B and A. The direction of all voltammograms was toward negative potentials first with a starting potential of 0 V. (a) Comparison of voltammograms obtained after the permeation measurement (RB was initially present in the phase A only, x = 100 μM, y = 0 μM) at a scan rate of 20 mV s^{-1} and membrane rotation of 200 rpm (21 rad s^{-1}) using 1,9-decadiene (black), NPOE (blue), ODCB (green), and 1-octanol (red) as SLM solvents. (b) Detailed voltammograms in the NPOE system at scan rates of 5, 10, 20, 40, 60, and 80 mV s^{-1}, corresponding to black, red, golden, green, blue, and violet curves, respectively. RB was initially present in both aqueous phases (x = y = 100 μM), and the membrane was not rotated. The gray curve represents a "blank" voltammogram, i.e., that for an analyte-free system (x = y = 0).

Second, the maximum aqueous concentration of RB^+ cation found from the dissociation equilibrium at pH 7.0 is ~0.05 μM (pK_a ~ 3.2−3.7), while the current corresponds to the concentration of the transferred ion of about 0.1−5 mM depending on the SLM solvent (from eq 4, below). This large concentration mismatch and the change of current with solvent strongly support the conclusion that the membrane rather than aqueous concentration drives the transfer.

Finally, the current response of the different solvent systems is proportional to the distribution coefficient between the SLM and aqueous phase. The increase in the distribution coefficient results in a higher concentration inside the membrane; however, the current also depends on the RB^+ diffusion within the membrane. A modified Randles-Ševčík equation, which relates the diffusion-limited transfer peak current, I_p, to the system properties, was derived by Samec et al. for the SLM system at 298 K:[8]

$$I_p = 0.3837\left(\frac{zF}{RT}\right)^{1/2} zFA_X {D_M}^{1/2} c_{i,M,X} \nu^{1/2} \quad (4)$$

where z is the charge of the transferred ion, F is the Faraday constant, A_X is the area of the relevant membrane surface corrected for porosity, D_M is the diffusion coefficient of the ion i in the membrane phase, $c_{i,M,X}$ is the membrane ionic concentration at the interface with phase X (A or B), and ν is the scan rate (note the dimensionless peak current function is 0.4463 for a reversible charge transfer across a single electrified interface). Combining the analytical (total) concentration of RB in the system obtained from UV−vis absorption and the ionic concentration calculated accurately from the measured current, eq 4 allows us to determine the dissociation equilibrium in the organic phase. Table 2 shows diffusion coefficients of RB in each solvent (calculated using the solvent viscosity, aqueous diffusion coefficient, and the Stokes−Einstein equation[30,43,46−48]) and the peak current values (peak 1 and 3). Equation 4 was used to calculate the effective ionic concentrations within the membrane at both interfaces: the corresponding concentrations on the aqueous sides of the interface were found from the distribution coefficients (Table 3). The concentrations determined imply that the membrane-to-aqueous transfer dominates the observed voltammetric response. Note that, for the stirred system (Figure 4a), the current−potential response of membrane-to-aqueous transfer (peaks 1 and 3) shows indications of a sigmoidal shape, indicating that stirring results in a quasi-linear concentration profile within the membrane. In contrast, the voltammograms recorded at scan rates between 5 and 80 mV s^{-1}, carried out in an unstirred NPOE supported liquid membrane system (Figure 4b), show a peak-shape current−potential response indicating linear diffusion on both sides of the membrane. Peaks 1 and 3 of Figure 4b were used for an accurate current−scan rate

Table 2. Viscosities, Membrane Diffusion Coefficients, Transfer Peak Currents, and Ionic Concentrations of Rhodamine B in the SLM System

SLM solvent	$\eta/10^{-3}$ Pa s^a	$D_M/10^{-6}$ cm s^{-2b}	$I_{p,1}/\mu A^c$	$I_{p,3}/\mu A^c$
ODCB	1.32	3.25	−149.05	198.12
NPOE	13.80	0.31	−54.91	69.35
1,9-decadiene	12.85	0.34	−7.62	7.49

[a]Membrane solvent viscosities taken from refs 30, 46, 48, and 50. [b]Membrane diffusion coefficient calculated from the Stokes−Einstein equation[43,47] using the viscosity ratios and an estimate of the RB aqueous diffusion coefficient based on its molar mass.[51] [c]Transfer peak current of peaks 1 and 3 from cyclic voltammetry (20 mV s^{-1}, Figure 4a,), respectively.

Table 3. Membrane and Aqueous Ionic Concentrations of Rhodamine B in the SLM System

SLM solvent	$c_{i,M,A}$/mM[a]	$c_{i,M,B}$/mM[a]	$c_{i,M}$/mM[b]	$c_{i,A}$/nM[c]	$c_{i,B}$/nM[c]
ODCB	5.69	3.24	4.47	12.48	0.07
NPOE	1.98	1.19	1.59	26.22	0.26
1,9-decadiene	0.22	0.16	0.19	45.22	19.35

[a]Membrane ionic concentrations at the interface with phases A and B, respectively (from eq 4). [b]Average membrane concentration calculated as an arithmetic average of $c_{i,M,B}$ and $c_{i,M,A}$. [c]Aqueous ionic concentrations in phases A and B, respectively (from the distribution equilibrium).

dx.doi.org/10.1021/ac402328w | Anal. Chem. 2014, 86, 435−442

gradient analysis using eq 4 (NPOE data in Table 3). The unusual behavior of partially charged species at the interface between two immiscible liquids, which has been described previously for a simple liquid−liquid system,[49] gives rise to a complex ionization and distribution equilibrium and hindered accurate quantitative analysis of rhodamine B in terms of the models for SLM transport, as further discussed in the Supporting Information (S-5).

The existence of the two pairs of transfer peaks observed in the voltammograms is now discussed. Each pair of peaks is attributed to transfer out of and back into the membrane phase at the relevant membrane interface, i.e., peaks 1 and 2 correspond to analyte transfer at M|B interface and peaks 3 and 4 to transfer at M|A interface, as indicated in Figure 4a. The double voltammetric transfer peak is a direct and logical consequence of the ionic transfer in systems with two interfaces; however, despite the considerable volume of literature on both experimental[7−11,14,25,52,53] and theoretical[12,13,54] membrane voltammetry, the majority of authors have not discussed this phenomenon. This is likely due to the analyte ions being present in only one of the aqueous phases, resulting in a single-pair of peaks in a voltammogram. Should one use an ion with substantial partitioning into the membrane, another pair of transfer peaks should be detectable, as shown for RB^+ in Figure 4a. Similarly, placing the analyte ion in both aqueous phases will result in double-transfer voltammetry, as shown below for multiple ions. To the best of our knowledge, the only description of this double-transfer voltammogram, which has important consequences for many membrane science applications, was given by Shirai et al., who provided a detailed analysis of the double-interface system and studied the effect of supporting electrolyte on the ion transfer using a 6-electrode setup with a 1 cm-thick nitrobenzene SLM.[14] Samec et al. reported voltammetric transfer of ionized species in an supported NPOE membrane, but only the positive half of the voltammogram was shown.[8] Similar results were reported by Ulmeanu et al.,[10] suggesting that the double transfer may have been observed previously, but a detailed description of this phenomenon was not given. Molina et al. derived a substantial theoretical body of work, supported with experiments, to describe voltammetry at membrane interfaces; however, only cases where fairly hydrophilic ions were present in one of the aqueous phases were considered, in contrast to the RB^+ case described above.[12,13,54]

The observed double-transfer voltammogram is a direct consequence of the existence of two interfaces and therefore two energy barriers that the ion has to overcome on transfer from aqueous phase A to B (or vice versa). The addition of a second ITIES in series has the effect of increasing the overall voltage of the system.[55−57] As a result, the potential window is doubled in comparison to a single ITIES interface system. When there is no potential difference between the two aqueous phases, the ions remain in their respective phases. On application of the potential difference, the ions will transfer in the relevant direction (cations toward the more negative phase and anions to the more positive phase). Figure 5 shows cyclic voltammograms obtained for a series of cations with differing standard Gibbs energies of transfer, which are present in both aqueous phases (except CrV^+), with a full series of analyzed species including anions given in the Supporting Information, S-6). Increasing hydrophilicity of the ions results in a requirement for an increasing cell voltage in order to transfer the ions across the respective interface, with the most

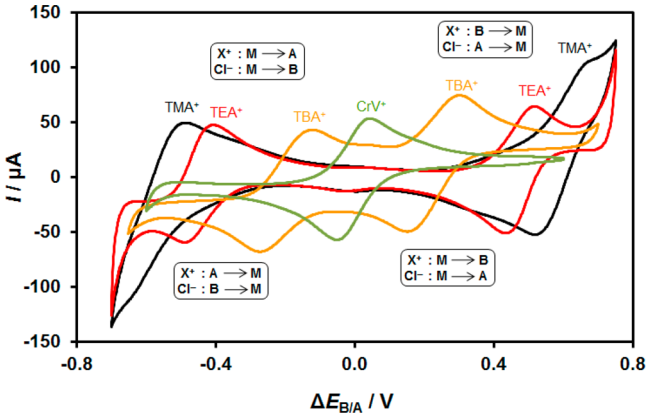

Figure 5. Cyclic voltammograms of transfer of selected cations in a NPOE supported liquid membrane system. The black, red, gold, and green curves denote tetramethylammonium (TMA^+), tetraethylammonium (TEA^+), tetrabutylammonium (TBA^+), and crystal violet (CrV^+) voltammograms, respectively. X^+ stands for any of the studied cations.

hydrophilic cation, tetramethylammonium, transferring near the positive and negative vertices of the potential window. The tetralkylammonium transfers are assumed to be coupled to the transfer of chloride ion across the other solution/membrane interface, as indicated in Figure 5. This observation may be rationalized by consideration of the Galvani potential distribution across the individual interfaces. A finite potential difference should be dropped equally across both interfaces (A|M and M|B) in a symmetrical system.[14] Therefore, the resultant potential window is extended by a factor of n, where n is the number of interfaces.

The half-wave potentials of transfer of the studied cations, $E_i^{1/2}$, are listed in Table 4. Data suggests that the half-wave

Table 4. Half-Wave Potentials and Peak Separations of Transfer of the Studied Cations[a]

	$E_i^{1/2}$/V		ΔE_p/V	
cation	neg	pos	neg	pos
TMA^+	−0.558	0.594	0.131	0.136
TEA^+	−0.449	0.477	0.079	0.079
TBA^+	−0.198	0.227	0.148	0.149
RB^+ (only A)	−0.437	0.482	0.120	0.117
RB^+ (A and B)	−0.458	0.495	0.100	0.091
CrV^+	−0.004		0.092	

[a]Both values for the peaks in the negative and positive branches of the voltammogram are shown (obtained from 40 mV s^{-1} scans).

potential values are reasonably symmetrical about the zero potential difference. Also, the order of the observed half-wave potentials is in agreement with the lipophilicity of the ions (standard Gibbs energy of transfer) reported by various groups.[30,58,59] The exact $E_i^{1/2}$ value, however, will depend not only on the standard transfer potentials across a single ITIES, $\Delta\phi_i^0$, of the cation and its counterion (chloride) but also on other parameters, and development of a suitable theoretical model is beyond the scope of this work. The half-wave potential formula for a system, where the studied cation is supplied only from one of the aqueous phases and compensating current flow at the other liquid−liquid interface is facilitated by organic electrolyte cation, has been derived by

dx.doi.org/10.1021/ac402328w | Anal. Chem. 2014, 86, 435−442

Samec et al.(eq 14 in[8]) and Molina et al.(eqs 21−23 in[54]): note, however, that there is a discrepancy between the diffusion coefficients used in the two papers. $E_i^{1/2}$ has been shown to depend on the standard transfer potentials across single ITIES, $\Delta\phi_i^0$, of the studied cation and its counterion (org. phase cation), their analytical concentrations and diffusion coefficients in both membrane and aqueous phase, and the Ohmic potential drop. The peak separation, ΔE_p, of 60 mV and dimensionless current of 1.13 for a symmetric system, where the studied ion is present in both aqueous phases surrounding a thick membrane, was suggested by Kakiuchi.[60] ΔE_p of tetraalkylammonium ions and RB transfer, however, ranges between 80 and 150 mV, and the dimensionless current varies between 0.209 and 0.346 as shown in Table 4. This is most likely due to the overlap of the two diffusion layers inside the thin membrane,[8,60] which is supported by the observed change of peak separation with scan rate (full table listing $E_i^{1/2}$ and ΔE_p values for all the studied ions is found in Supporting Information, S-6).

In contrast to tetraalkylammonium ions, crystal violet has only been added to one of the aqueous phases (A), which results in a single pair of voltammetric peaks as reported in the literature referred to above. The peak separation and the dimensionless peak current on the forward scan have been determined as 92 mV and 0.349, respectively, in reasonable agreement with the theoretical values (91 mV and 0.384, respectively) derived for this asymmetric system.[8] Furthermore, the lipophilic CrV^+ (which has in fact been used as an organic phase electrolyte by various group; the absolute value of its standard Gibbs energy of transfer is close to that of chloride[61,62]) is readily transferred to the membrane phase, and the observed half-wave potential of the coupled transfer is close to zero ($E_i^{1/2} = -4$ mV).

The observed double-transfer of ions across the double ITIES has important consequences for membrane applications such as separation, purification, or extraction of anions and cations.[5,63,64] Due to the reversibility of the transfer, both membrane and aqueous phases can be used as donor or acceptor phases in these applications. For example, a mixture of ions can be separated depending on the ions' lipophilicity and thereby concentrated in one of the phases. This could be done either in an aqueous−organic−aqueous or an organic−aqueous−organic configuration depending on the particular application. As demonstrated above, the transfer of the analyte is not restricted to only one of the liquid−liquid interfaces and electrochemistry can be used to control analyte distribution in all three liquid phases. Furthermore, the supported liquid systems not only are restricted to use of one membrane with two liquid−liquid interfaces but also can be constructed in series, similar to battery construction, increasing the contact surface area between the two phases and therefore transfer efficiency, which is particular appealing when used in a flow or microfluidic configuration.[65−68] The exploitation of potential SLM applications has already proven of significant interest in research areas such as drug extraction,[1] purification processes,[69] microreaction apparatus for synthetic chemistry,[70] concentration of analytes in order to increase the limit of detection,[71] separation of heavy metals/radioactive elements,[72,73] or leaching of metal ions from ore.[74]

CONCLUSIONS

A voltammetric and spectrophotometric study of rhodamine B transfer across the supported liquid membrane, separating two aqueous phases, is presented. The data obtained from both analytical methods is used to determine the concentration profile of rhodamine B cations and its uncharged form across the aqueous−membrane−aqueous layers. Application of a potential difference between the two aqueous phases and measurement of the transfer current indicate that, for a lipophilic species such as rhodamine B, the transfer is driven in the "out of membrane" direction, due to its high membrane concentration and limited availability of ions in the aqueous phases. Most interestingly, a double-transfer peak is observed for rhodamine B voltammetry, indicating two separate transfers occur at each liquid−liquid interface depending on the polarity of the applied potential difference. Surprisingly, with the exception of one research group,[14] this feature has not been described in the literature and requires refinement of existing models of ion transfer across SLMs.

The approach described has important consequences for SLM applications such as electrically modulated extraction, separation, and purification of ions and in many other areas. The membrane composition and potential window can be fine-tuned to the ion of interest and, depending on its lipophilicity, either membrane or aqueous phases can be used as the target phase in which ions are concentrated. Particularly attractive is the idea of an "electrochemical switch" where lipophilic ions, such as rhodamine B, can be trafficked to either side of the membrane, simply by changing the polarity of the voltage source. This concept is not limited to systems with one SLM but can be extended to a series of membranes, for example, in a linear flow system, allowing complex mixtures of ions to be processed effectively. Furthermore, cations and anions can be separated in one step and concentrated in separate phases. Clearly, this setup can be reversed to an organic−aqueous membrane−organic arrangement and similar methods applied to more hydrophilic ions.

ASSOCIATED CONTENT

Supporting Information

Additional information as noted in text. This material is available free of charge via the Internet at http://pubs.acs.org.

AUTHOR INFORMATION

Corresponding Author

*Tel: +44 (0)161-306-4522. Fax: +44 (0)161-275-4598. E-mail: robert.dryfe@manchester.ac.uk.

Notes

The authors declare no competing financial interest.

ACKNOWLEDGMENTS

We thank EPSRC for funding for M.V.

REFERENCES

(1) Pedersen-Bjergaard, S.; Rasmussen, K. E. *J. Chromatogr., A* **2006**, *1109*, 183−190.
(2) Buck, R. P.; Lindner, E. *Anal. Chem.* **2001**, *73*, 88A−97A.
(3) Kansy, M.; Senner, F.; Gubernator, K. *J. Med. Chem.* **1998**, *41*, 1007−1010.
(4) Ramanujam, A.; Dhami, P. S.; Gopalakrishnan, V.; Dudwadkar, N. L.; Chitnis, R. R.; Mathur, J. N. *Sep. Sci. Technol.* **1999**, *34*, 1717−1728.
(5) Pedersen-Bjergaard, S.; Rasmussen, K. E. *Anal. Bioanal. Chem.* **2007**, *388*, 521−523.
(6) Samec, Z. *Pure Appl. Chem.* **2004**, *76*, 2147−2180.
(7) Samec, Z.; Trojánek, A.; Langmaier, J.; Samcová, E.; Málek, J. *Electroanalysis* **2000**, *12*, 901−904.

(8) Samec, Z.; Trojánek, A.; Langmaier, J.; Samcová, E. *J. Electroanal. Chem.* **2000**, *481*, 1−6.
(9) Ulmeanu, S. M.; Jensen, H.; Bouchard, G.; Carrupt, P. A.; Girault, H. H. *Pharm. Res.* **2003**, *20*, 1317−1322.
(10) Ulmeanu, S. M.; Jensen, H.; Samec, Z.; Bouchard, G.; Carrupt, P. A.; Girault, H. H. *J. Electroanal. Chem.* **2002**, *530*, 10−15.
(11) Murtomäki, L.; Barker, M. H.; Manzanares, J. A.; Kontturi, K. *J. Electroanal. Chem.* **2003**, *560*, 95−103.
(12) Molina, A.; Ortuño, J. A.; Serna, C.; Torralba, E.; Gonzalez, J. *Electroanalysis* **2009**, *22*, 1634−1642.
(13) Molina, A.; Serna, C.; Ortuño, J. A.; Gonzalez, J.; Torralba, E.; Gil, A. *Anal. Chem.* **2009**, *81*, 4220−4225.
(14) Shirai, O.; Kihara, S.; Yoshida, Y.; Matsui, M. *J. Electroanal. Chem.* **1995**, *389*, 61−70.
(15) Bakker, E.; Bühlmann, P.; Pretsch, E. *Electroanalysis* **1999**, *11*, 915−933.
(16) Choi, Y. W.; Moon, S. H. *Environ. Monit. Assess.* **2001**, *70*, 167−180.
(17) Abraham, M. H.; Chadha, H. S.; Leitao, R. A. E.; Mitchell, R. C.; Lambert, W. J.; Kaliszan, R.; Nasal, A.; Haber, P. *J. Chromatogr., A* **1997**, *766*, 35−47.
(18) Faller, B.; Grimm, H. P.; Loeuillet-Ritzler, F.; Arnold, S.; Briand, X. *J. Med. Chem.* **2005**, *48*, 2571−2576.
(19) Bouchard, G.; Galland, A.; Carrupt, P. A.; Gulaboski, R.; Mirceski, V.; Scholz, F.; Girault, H. H. *Phys. Chem. Chem. Phys.* **2003**, *5*, 3748−3751.
(20) Jing, P.; Zhang, M.; Hu, H.; Xu, X.; Liang, Z.; Li, B.; Shen, L.; Xie, S.; Pereira, C. M.; Shao, Y. *Angew. Chem., Int. Ed.* **2006**, *45*, 6861−6864.
(21) Sabela, A.; Marecek, V.; Samec, Z.; Fuoco, R. *Electrochim. Acta* **1992**, *37*, 231−235.
(22) Shao, Y.; Stewart, A. A.; Girault, H. H. *J. Chem. Soc., Faraday Trans.* **1991**, *87*, 2593−2597.
(23) Duffey, M. E.; Fennell Evans, D.; Cussler, E. L. *J. Membr. Sci.* **1978**, *3*, 1−14.
(24) Mackova, J.; Mikulaj, V.; Rajec, P. *J. Radioanal. Nucl. Chem.* **1994**, *183*, 85−91.
(25) Langmaier, J.; Samec, Z. *Electrochem. Commun.* **2007**, *9*, 2633−2638.
(26) Mayer, P. T.; Anderson, B. D. *J. Pharm. Sci.* **2002**, *91*, 640−646.
(27) Velický, M.; Bradley, D. F.; Tam, K. Y.; Dryfe, R. A. W. *Pharm. Res.* **2010**, *27*, 1644−1658.
(28) Velický, M.; Tam, K. Y.; Dryfe, R. A. W. *Eur. J. Pharm. Sci.* **2011**, *44*, 299−309.
(29) Velický, M.; Tam, K. Y.; Dryfe, R. A. W. *Anal. Chem.* **2012**, *84*, 2541−2547.
(30) Samec, Z.; Langmaier, J.; Trojánek, A. *J. Electroanal. Chem.* **1996**, *409*, 1−7.
(31) Seidi, S.; Yamini, Y.; Baheri, T.; Feizbakhsh, R. *J. Chromatogr., A* **2011**, *1218*, 3958−3965.
(32) Xiao, K. P.; Bühlmann, P.; Nishizawa, S.; Amemiya, S.; Umezawa, Y. *Anal. Chem.* **1997**, *69*, 1038−1044.
(33) Ottaviani, G.; Martel, S.; Escarala, C.; Nicolle, E.; Carrupt, P. A. *Eur. J. Pharm. Sci.* **2008**, *35*, 68−75.
(34) Fujii, K.; Tanibuchi, S.; Kihara, S. *Anal. Sci.* **2005**, *21*, 1415−1420.
(35) González-Buitrago, J. M.; González, C. *Clin. Chim. Acta* **2006**, *365*, 50−57.
(36) Lundgren, H. P.; Binkley, C. H. *J. Polym. Sci.* **1954**, *14*, 139−158.
(37) Moczko, E.; Cauchi, M.; Turner, C.; Meglinski, I.; Piletsky, S. *IEEE Trans. Biomed. Eng.* **2011**, *58*, 2154−2160.
(38) Robison, A. D.; Huang, D.; Jung, H.; Cremer, P. S. *Biointerphases* **2013**, *8*, 1−9.
(39) Fischer, H.; Kansy, M.; Avdeef, A.; Senner, F. *Eur. J. Pharm. Sci.* **2007**, *31*, 32−42.
(40) Muthuraman, G.; Teng, T. T. *Desalination* **2009**, *249*, 1062−1066.
(41) McHedlov-Petrossyan, N. O.; Kukhtik, V. I.; Alekseeva, V. I. *Dyes Pigm.* **1994**, *24*, 11−35.
(42) Woislawski, S. *J. Am. Chem. Soc.* **1953**, *75*, 5201−5203.
(43) Culbertson, C. T.; Jacobson, S. C.; Michael Ramsey, J. *Talanta* **2002**, *56*, 365−373.
(44) Tam, K. Y.; Velický, M.; Dryfe, R. A. W. In *Physico-Chemical Methods in Drug Discovery and Development*; Mandić, Z., Ed.; IAPC Publishing: Zagreb, 2012.
(45) Bard, A. J.; Faulkner, L. R. *Electrochemical Methods. Fundamentals and Applications*, 2nd ed.; John Wiley & Sons, Inc.: New York, 2001.
(46) Baragi, J. G.; Aralaguppi, M. I.; Aminabhavi, T. M.; Kariduraganavar, M. Y.; Kulkarni, S. S. *J. Chem. Eng. Data* **2005**, *50*, 917−923.
(47) Dean, R. B.; Loring, H. S. *J. Biol. Chem.* **1945**, *157*, 717−721.
(48) Velický, M.. PhD Thesis, University of Manchester, 2011.
(49) Velický, M.; Tam, K. Y.; Dryfe, R. A. W. *J. Electroanal. Chem.* **2012**, *683*, 94−102.
(50) Lide, D. R. *Handbook of Chemistry and Physics*, 87th ed.; CRC Press: Boca Raton, FL, 1998.
(51) Avdeef, A. *Expert Opin. Drug Metab. Toxicol.* **2005**, *1*, 325−342.
(52) Barker, M. H.; Murtomäki, L.; Kontturi, K. *J. Electroanal. Chem.* **2001**, *497*, 61−68.
(53) Samec, Z.; Langmaier, J.; Trojánek, A.; Samcová, E.; Málek, J. *Anal. Sci.* **1998**, *14*, 35−41.
(54) Molina, A.; Serna, C.; Gonzalez, J.; Ortuño, J. A.; Torralba, E. *Phys. Chem. Chem. Phys.* **2009**, *11*, 1159−1166.
(55) Guerrette, J. P.; Oja, S. M.; Zhang, B. *Anal. Chem.* **2012**, *84*, 1609−1616.
(56) Loget, G.; Roche, J.; Kuhn, A. *Adv. Mater.* **2012**, *24*, 5111−5116.
(57) Plana, D.; Jones, F. G. E.; Dryfe, R. A. W. *J. Electroanal. Chem.* **2010**, *646*, 107−113.
(58) Chrisstoffels, L. A. J.; De Jong, F.; Reinhoudt, D. N. *Chem.—Eur. J.* **2000**, *6*, 1376−1385.
(59) Wilke, S.; Zerihun, T. *J. Electroanal. Chem.* **2001**, *515*, 52−60.
(60) Kakiuchi, T. *Electrochim. Acta* **1998**, *44*, 171−179.
(61) Vaný sek, P.; Hernandez, I. C.; Xu, J. *J. Colloid Interface Sci.* **1990**, *139*, 527−534.
(62) Sun, Z.; Wang, E. *Electroanalysis* **1989**, *1*, 507−515.
(63) Collins, C. J.; Berduque, A.; Arrigan, D. W. M. *Anal. Chem.* **2008**, *80*, 8102−8108.
(64) Kusumocahyo, S. P.; Kanamori, T.; Sumaru, K.; Aomatsu, S.; Matsuyama, H.; Teramoto, M.; Shinbo, T. *J. Membr. Sci.* **2004**, *244*, 251−257.
(65) Berduque, A.; Sherburn, A.; Ghita, M.; Dryfe, R. A. W.; Arrigan, D. W. M. *Anal. Chem.* **2005**, *77*, 7310−7318.
(66) Oelke, J.; Kaindl, T.; Pasc, A.; Guttenberg, Z.; Wixforth, A.; Tanaka, M. *Materials* **2013**, *6*, 669−681.
(67) Petersen, N. J.; Foss, S. T.; Jensen, H.; Hansen, S. H.; Skonberg, C.; Snakenborg, D.; Kutter, J. P.; Pedersen-Bjergaard, S. *Anal. Chem.* **2011**, *83*, 44−51.
(68) Wang, X.; Saridara, C.; Mitra, S. *Anal. Chim. Acta* **2005**, *543*, 92−98.
(69) Msagati, T. A. M.; Mamba, B. B. *Phys. Chem. Earth* **2011**, *36*, 1167−1177.
(70) Xu, B. B.; Zhang, Y. L.; Wei, S.; Ding, H.; Sun, H. B. *ChemCatChem* **2013**, *5*, 2091−2099.
(71) Kubáň, P.; Šlampová, A.; Boček, P. *Electrophoresis* **2010**, *31*, 768−785.
(72) Ambashta, R. D.; Sillanpää, M. E. T. *J. Environ. Radioact.* **2012**, *105*, 76−84.
(73) Chen, Y.; Zhang, Y.; Li, X.; Wang, W.; He, T. *Prog. Chem.* **2011**, *23*, 1033−1040.
(74) Adebayo, A. O.; Sarangi, K. *Sep. Purif. Technol.* **2008**, *63*, 392−399.